Article

Demonstrating Structural Deformation in an Inorganic Nanotube

Yuri G. Andreev, and Peter G. Bruce

J. Am. Chem. Soc., **2008**, 130 (30), 9931-9934 • DOI: 10.1021/ja8028334 • Publication Date (Web): 01 July 2008

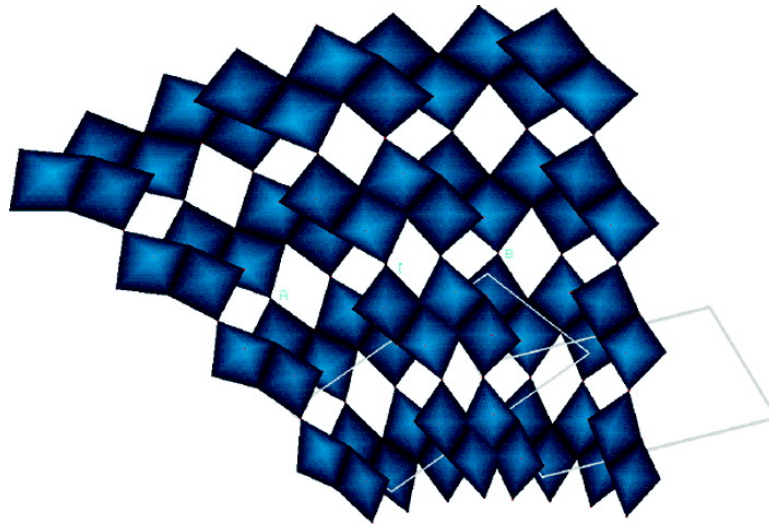

J|A|C|S
ARTICLES

Published on Web 07/01/2008

Demonstrating Structural Deformation in an Inorganic Nanotube

Yuri G. Andreev and Peter G. Bruce*

School of Chemistry, University of St. Andrews, St. Andrews, Fife KY16 9ST, Scotland

Received April 17, 2008; E-mail: p.g.bruce@st-and.ac.uk

Abstract: There is much current interest in nanostructured materials (nanotubes, nanobelts, nanospheres, etc.). Their crystal structures can differ from those of the equivalent bulk materials. Determining these differences is important in understanding how the properties of nanomaterials differ from those of the bulk. Established methods of X-ray structure determination become increasingly difficult or impossible to apply on reducing the dimensions to a few nanometers. Here we show that, by combining the Debye equation for X-ray scattering (which relates an ensemble of atoms to their diffraction pattern without recourse to symmetry) with a model of the crystal structure, generated by folding the ideal crystal structure into a nanotube, the severely broadened/distored powder diffraction pattern may be described. This procedure reveals the significant structural deformations necessary to accommodate the nanotube shape. The importance of knowing the (deformed) crystal structure is discussed.

1. Introduction

Knowledge of structure is the foundation of modern chemistry. The structures of nanomaterials can differ significantly from their bulk counterparts; the stability of different polymorphs can even be reversed.[1] However, determining the atomic structure of nanomaterials can be difficult because established crystallographic techniques rely on long-range translational symmetry. Yet establishing such structure is very important in order to explain the often unique optical, magnetic, and electrical properties of nanomaterials. For materials with particle sizes of only a few nanometers, the peaks in their powder diffraction patterns become severely, and often anisotropically, broadened, rendering the application of established crystallographic methods difficult or impossible.[2,3] Attempts are being made to circumvent the use of such methods by analyzing total scattering or by using the Debye equation, neither of which requires any assumption of translational symmetry.[4,5]

Problems of structure elucidation apply to all nanomaterials, but the situation is particularly difficult for anisotropic nanoparticles, hereafter referred to as nanoshaped materials, such as inorganic nanotubes discussed here. Not only are their powder patterns severely broadened due to their nanometer dimensions (see Figure 1), but in addition the ideal crystal structure is expected to distort as it curves to form the nanotube, introducing further peak broadening in the powder diffraction pattern.

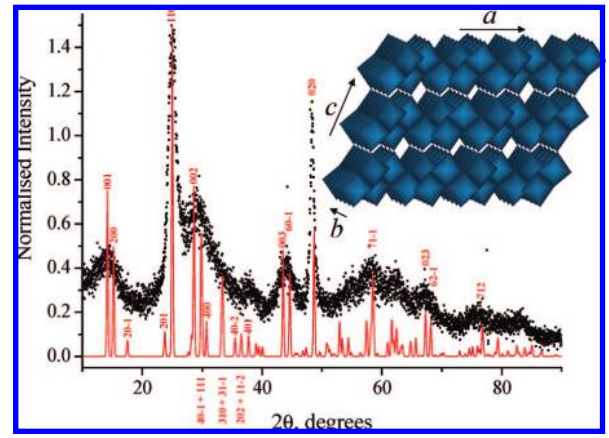

Figure 1. X-ray diffraction pattern of TiO_2−B nanotubes: dots, observed pattern; red line, simulated pattern based on the ideal TiO_2−B structure. Numbers are Miller indices. Inset shows an ideal TiO_2−B crystal structure with crystallographic axes.

Attention is becoming increasingly focused on the important problem of establishing the arrangement of atoms in nanosized materials. However, elucidating the atomic structure of nanomaterials, especially those with considerably anisotropic morphologies (nanoflakes, nanotubes, nanobelts) and dimensions of a few nanometers, remains a formidable task.

Here we take an inorganic nanotube (illustrated using TiO_2−B nanotubes), and, by folding a slab of the ideal crystal structure (TiO_2−B) into a tube and then generating the powder pattern using the Debye equation (which directly relates atomic positions to the diffracted intensity), the severely broadened experimental powder diffraction pattern is reproduced. The structure is significantly distorted compared to that of the bulk material. The importance of knowing the true (distorted)

(1) Zhang, H.; Banfield, J. F. *J. Mater. Chem.* **1998**, *8*, 2073.
(2) Billinge, S. J. L.; Levin, I. *Science* **2007**, *316*, 561.
(3) Stephens, P. W. *J. Appl. Crystallogr.* **1999**, *32*, 281.
(4) (a) McGreevy, R. L.; Pusztai, L. *Mol. Simul.* **1988**, *1*, 359. (b) Petkov, V.; Billinge, S. J. L.; Shastri, S. D.; Himmel, B. *J. Non-Cryst. Solids* **2001**, *293*, 726. (c) Koloczek, J.; Burian, A. *J. Alloys Compd.* **2004**, *382* (1−2), 123. (d) Koloczek, J.; Hawelek, L.; Burian, A.; Dore, J. C.; Honkimäki, V.; Kyotani, T. *J. Alloys Compd.* **2005**, *401*, 46. (e) Oddershede, J.; Ståhl, K. *Z. Kristallogr. Suppl.* **2006**, *23*, 325. (f) Juhás, P.; Cherba, D. M.; Duxbury, P. M.; Punch, W. F.; Billinge, S. J. L. *Nature* **2006**, *440*, 655.
(5) (a) Gateshki, M.; Chen, Q.; Peng, L.-M.; Chupas, P.; Petkov, V. *Z. Kristallogr.* **2007**, *222*, 612. (b) Pradhan, S. K.; Mao, Y.; Wong, S. S.; Chupas, P.; Petkov., V. *Chem. Mater.* **2007**, *19*, 6180.

structure of a nanostructured material for understanding its unique properties is illustrated.

2. Results and Discussion

2.1. The Powder Diffraction Pattern. Nanoshaped materials (e.g., nanotubes, nanobelts, nanospheres) exhibit unique and important optical, magnetic, and electrical properties.[6,7] Of the various nanoshaped materials, nanotubes are arguably the most significant and intensively studied. Inorganic nanotubes, e.g. MoS_2, WS_2, were first reported by Tenne.[8] Their greater compositional and structural complexity compared with carbon nanotubes results in a wealth of important properties. However, understanding such properties relies on knowing the crystal structure, something that their greater structural complexity renders more challenging than for carbon nanotubes. Interest in such inorganic nanotubes has grown rapidly in recent years, with many examples now known, e.g., MoO_3, V_2O_5, TiS_2.[6,9] Titanium dioxide is one of the most important inorganic compounds with applications as pigments, in catalysis, in solar energy conversion, etc.[9] Since the discovery of titanium dioxide nanotubes, interest in such materials has been intense.[11] The work of many groups is summarized in a recent review.[12] TiO_2−B, the fifth polymorph of titanium dioxide, can be easily prepared in the form of nanotubes with high purity and in high yield, with internal and external diameters of ∼5 and ∼10 nm, respectively, that can be up to tens of micrometers long.[13,14] These nanotubes have been shown to exhibit superior properties compared with the equivalent bulk material.[14]

A powder X-ray diffraction pattern for the TiO_2−B tubes is presented in Figure 1, along with the ideal monoclinic TiO_2−B crystal structure. The latter consists of layers formed from edge-sharing TiO_6 octahedra lying in the *ab* plane of the unit cell and stacked along *c* such that only the corners of the TiO_6 link adjacent layers (Figure 1). A detailed description of the TiO_2−B crystal structure can be found in ref 15. A simulated powder X-ray diffraction pattern based on the crystal structure of bulk TiO_2−B is shown in Figure 1, from which the previous assignment of the crystal structure to that of TiO_2−B is confirmed.[14] However, comparison between the simulated and observed powder patterns highlights the severe *hkl*-dependent peak broadening/distortion of the latter, features that reflect the limited dimensions of the tube walls, the anisotropy of the nanotubes, and the structural distortions (deviations from the ideal crystal structure) which are expected to occur on bending a layered crystal structure into a nanotube. The broadened and distorted peaks make analysis of the diffraction data by established crystallographic methods much more challenging than for micrometer-sized dimensions. In established approaches, the peak intensities are related to the ideal crystal structure, whereas the peak shape is determined by a convolution of sample peak broadening, due mainly to the crystallite size and microstrains, and instrument broadening. The last of these becomes negligible for particle sizes of a few nanometers, as is the case for the TiO_2−B nanotubes. Size−strain refinement has been incorporated into the Rietveld method of structure refinement and applied to materials with moderate peak broadening and limited anisotropy of crystallite size and strains using either a physical model or a phenomenological approach to describe peaks shapes.[3,16] Severely broadened diffraction patterns, like the one from the monoclinic TiO_2−B nanotubes shown in Figure 1, require a different approach in order to extract the (distorted) crystal structure.

2.2. Application of the Debye Approach. Debye, in 1915, derived an equation that directly relates the interatomic distances between each pair of atoms in the scattering volume to the observed X-ray diffraction pattern, without recourse to symmetry (crystallography).[17] The equation is exact in the first Born, or kinematic, approximation and deals explicitly with Bragg and diffuse scattering as well as the small-angle scattering from a powder. The intensity of X-ray radiation diffracted by an array of atoms, allowing all orientations of the array to have equal probability, is

$$I(\theta) = \sum_n f_n^2(\theta) + 2\sum_i \sum_j f_i(\theta) f_j(\theta) [\sin(4\pi r_{ij} \sin\theta/\lambda)/(4\pi r_{ij} \sin\theta/\lambda)]$$

where $f_n(\theta)$ is the atomic form-factor of the *n*th atom in the array, λ is the wavelength, and r_{ij} is the distance between atoms *i* and *j*. To account for the effect of preferred orientation, we have employed a multiplier, T_{ij}, in the double sum of the above equation:

$$T_{ij} = \left(T^2 \cos^2 \alpha_{ij} + \frac{1}{T}\sin^2 \alpha_{ij}\right)^{-3/2}$$

The correction is similar to the March−Dollase formulation;[18] however, in this case r_{ij} is the angle between α_{ij} and the preferred orientation vector (the [010] direction in the case of TiO_2−B nanotubes). *T* is the adjustable preferred orientation parameter.

Simply by applying this equation to a structural model for TiO_2−B nanotubes, constructed as described below, it is possible to simulate the complete powder diffraction profile and hence elucidate the deformed crystal structure.

A nanotube can be formed, for example, by folding the *ab* planes of the ideal TiO_2−B structure along the *a* axis, with the *b* and *c* axes placed along the axial and radial directions of the tube, respectively. First, the content of a single unit cell is translated along the *c* axis to achieve the desired wall thickness, *d*, and the coordinates of atoms in the thus-obtained fragment are transformed into a Cartesian frame (*x* axis along *a*, *y* along *b*, *z* completes right-handed orthogonal set). After that, all the atoms in the fragment are placed along radial directions of the

(6) Tenne, R.; Rao, C. N, R. *Phil. Trans. R. Soc. London A* **2004**, *362*, 2099.
(7) (a) Lee, K. Y.; Lim, J. R.; Rho, H.; Choi, Y. J.; Choi, K. J.; Park, J. G. *Appl. Phys. Lett.* **2007**, *91*, 201901. (b) Ma, H.; Cheng, F.; Chen, J.-Y.; Zhao, J.-Z.; Li, C.-S.; Tao, Z.-L.; Liang, J. *Adv. Mater.* **2007**, *19*, 4067.
(8) (a) Feldman, Y.; Wasserman, E.; Srolovitz, D. J.; Tenne, R. *Science* **1995**, *267*, 222. (b) Rothschild, A.; Frey, G. L.; Homyonfer, M.; Tenne, R. *Mater. Res. Innovations* **1999**, *3*, 145.
(9) (a) Satishkumar, B. C.; Govindaraj, A.; Vogl, E. M.; Basumallick, L.; Rao, C. N. R. *J. Mater. Res.* **1997**, *12*, 604. (b) Spahr, M. E.; Bitterli, P.; Nesper, R.; Muller, M.; Krumeich, F.; Nissen, H. U. *Angew. Chem., Int. Ed.* **1998**, *37*, 1263.
(10) (a) Matsuda, S.; Kato, A. *Appl. Catal.* **1983**, *8*, 149. (b) Hagfeldt, A.; Gratzel, M. *Chem. Rev.* **1995**, *95*, 49.
(11) Kasuga, T.; Hiramatsu, M.; Hoson, A.; Sekino, T.; Niichara, K. *Langmuir* **1998**, *14*, 3160.
(12) Ou, H. H.; Lo, S. L. *Sep. Purif. Technol.* **2007**, *58*, 179.
(13) Suzuki, Y.; Yoshikawa, S. *J. Mater. Res.* **2004**, *19*, 982.
(14) Armstrong, G.; Armstrong, A. R.; Canales, J.; Bruce, P. G. *Chem. Commun.* **2005**, 2454.
(15) Feist, T. P.; Davies, P. K. *J. Solid State Chem.* **1992**, *101*, 275.
(16) (a) Rietveld, H. M. *J. Appl. Crystallogr.* **1969**, *2*, 65. (b) *The Rietveld Method*; Young, R. A. Ed.; Oxford University Press: Oxford, 1993. (c) Lutterotti, L.;; Scardi, P. *J. Appl. Crystallogr.* **1990**, *23*, 246.
(17) Debye, P. *Ann. Phys.* **1915**, *351*, 809.
(18) Dollase, W. A. *J. Appl. Crystallogr.* **1986**, *19*, 267.

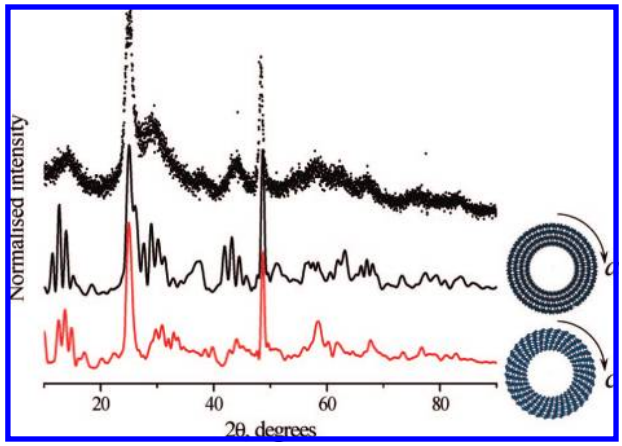

Figure 2. X-ray diffraction patterns of TiO_2−B nanotubes: dots, observed pattern; black line, simulated pattern based on folding the *ab* plane of the ideal TiO_2−B structure along *a* into a tube; red line, simulated pattern based on folding the *bc* plane of the ideal TiO_2−B structure along *c* into a tube. Views along the tube axis for each model are also shown.

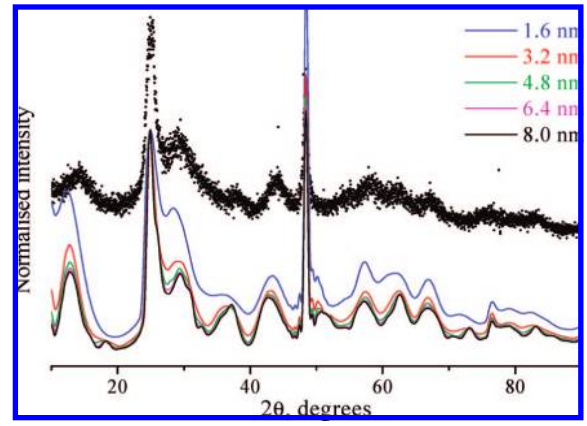

Figure 3. X-ray diffraction pattern of TiO_2−B nanotubes: dots, observed pattern; lines, simulated pattern based on folding the *ab* plane of the ideal TiO_2−B structure along *a* into segments of the tube of different length around the circumference of the outer wall of the nanotube. Each segment consists of four layers in the radial direction. Numbers indicate the lengths of the segments around the circumference.

tube at distances $R + z_i$ from the center (R is the inner radius of the tube, z_i is the coordinate of the ith atom). Angles between the radial directions are chosen to maintain the interatomic distances along x in the ideal structure on the circumference of the circle with the radius $R + d/2$. This ensures that the interatomic distances along the annulus of the tube, when averaged along the radial direction, are the same as in the bulk crystal structure. The created tube segment is then rotated around the tube center, filling the entire annulus. A seamless junction at the full circle is achieved by adjusting slightly the inner tube radius. Finally, the content of the one-unit-cell thick segment is translated along y, to achieve the desired length of the tube.

2.3. Structure and Implications. The 020 reflection in Figure 1 is noticeably narrower than other peaks, and, by application of the Scherrer formula, a coherence length in the *b* direction is estimated at 14.4 nm. This exceeds the diameter of the tubes and implies that the *b*-axis lies along the axial direction of the nanotubes, in accord with previous transition electron microscopy (TEM) studies.[14] Many materials have been formed as nanotubes, the vast majority of which are based on layered structures in which the layers fold to form the tubes.[6,19] Since the layers of the TiO_2−B structure lie in the *ab* plane, and since *b* lies along the axial direction, a tube may be formed by folding the *ab* plane along *a*, as shown in Figure 2 (middle pattern). Such a structure is consistent with the TEM image, which indicates that the walls are composed of four layers, consistent with the wall thickness of ∼2.5 nm.[14] Hence, the first structural model to be constructed was based on folding four layers of the crystal structure in the *ab* plane, as just described. The length of the tube was set at 14.2 nm (equivalent to 38 unit cells along *b* in the ideal structure), consistent with the coherence length along *b*, and the internal diameter at 2.3 nm, consistent the previous TEM data.[14] Bending a slab of the ideal TiO_2−B structure into a tube inevitably leads to distortions of the TiO_6 octahedra along the annulus of the tube. The maximum change in the corresponding Ti−O bond lengths is below the previously reported value.[20]

A powder diffraction pattern generated from this model is compared with experiment in Figure 2, from which it is clear that the model does not adequately describe the nanotubes. The peaks of the simulation are narrower and more abundant than in the observed powder diffraction pattern, suggesting that the model possesses more symmetry than is the case in practice. Similar problems are noted for an alternative model in which the tubes are formed by folding the *bc* plane along *c* (Figure 2, red line). Despite the inadequacies of both models, comparison between them and the observed powder diffraction pattern suggests that folding along *a* better describes the nanotubes. Also, as discussed above, folding along *a* is more physically reasonable than folding along *c*.

Recognizing that a model involving order throughout the entire nanotube does not adequately describe the observed data, segments of this structure were considered, all retaining four layers in the radial direction and extending 14.2 nm along *b* but extending to different degrees along the circumference. Powder X-ray diffraction patterns were calculated for such segments, ranging in size (along the circumference of the outer wall of the nanotube) from 1.6 to 10.2 nm (Figure 3). Careful examination of Figure 3 reveals that a segment of dimension 3.2 nm best represents the observed data. A schematic representation of a segment within the tube is shown in Figure 4; the segments are not in registry with each other but are aligned along the axial direction of the tubes. A segment of 1.6 nm is clearly inadequate, and that of 4.8 nm already begins to deviate from the observed pattern, as evident by examining the 2θ regions of 25−27° and 70−75°. Segments with three and five layers in the radial direction were also considered but provided a significantly inferior match to the observed data and, of course, are inconsistent with the thickness of the walls extracted from TEM. A powder pattern for an ideal TiO_2−B crystal structure (i.e., not curved to form the nanotube) with the same number of atoms as in the segment, which provides the best description to the powder data (3.2 nm), clearly shows that such an ideal structure is not satisfactory (Figure 4). An alternative model, in which the wall of the TiO_2−B nanotube is formed by layers of edge-sharing TiO_6 octahedra placed along the turns of an Archimedean (equidistant turns) spiral, has also been tested. The spiral model causes moderate distortions of the TiO_6 octahedra and has been successfully applied to anatase nanotubes.[5] However, the inevitable loss of registry in the radial direction, noted during the investigation of anatase nanotubes,[5b] is even

(19) Tenne, R. *Nat. Nanotechnol.* **2006**, *1*, 103.
(20) Park, K. T.; Pan, M. H.; Meunier, V.; Plummer, E. W. *Phys. Rev. Lett.* **2006**, *90*, 226105.

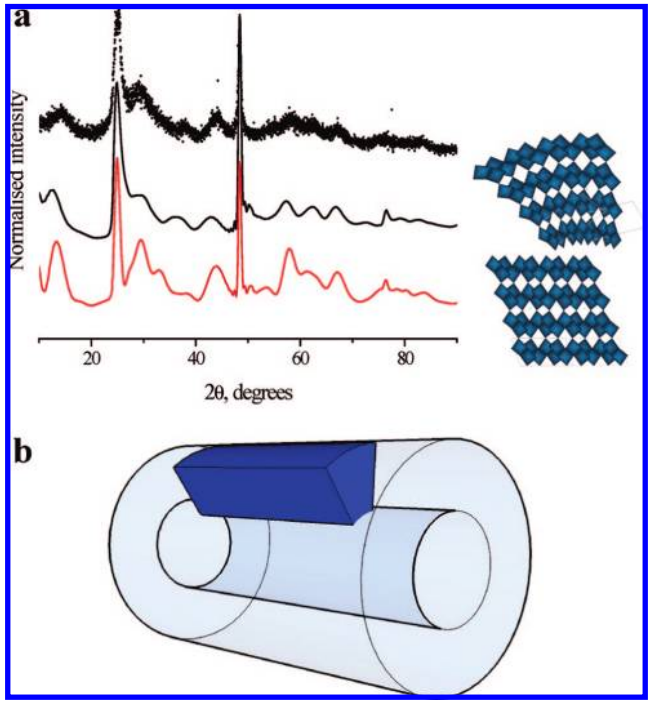

Figure 4. (a) X-ray diffraction pattern of TiO_2−B nanotubes: dots, observed pattern; black line, simulated pattern of a 3.2 nm tube segment corrected for preferred orientation; red line, simulated pattern of an ideal TiO_2−B crystal structure (i.e., not distorted to form the tube) with the same number of atoms as the segment. Views along *y* (*b* in case of the ideal structure) for model are also shown. (b) Schematic representation of an ordered segment within a nanotube.

more pronounced in TiO_2−B nanotubes, leading to a significant mismatch between the observed and calculated patterns. The spiral model does not adequately describe the TiO_2−B nanotubes.

Powders composed of particles with extreme aspect ratios often exhibit preferred orientation. Such an effect has been taken into account here for the TiO_2−B nanotubes to further improve the simulation of the powder diffraction data. Various degrees of preferred orientation were examined, and the best description of the observed powder diffraction data was obtained for a preferred orientation parameter of 0.8 (see Figure 4). In excess of 90% of the TiO_2−B powder is composed of nanotubes;[14] however other morphologies may affect the profile, precluding refinement of the structure, hence, a precise representation of the observed powder pattern cannot be expected. Yet the simulation reproduces well the main features of the powder diffraction pattern, in particular the severe *hkl*-dependent broadening.

The importance of knowing the true (distorted) crystal structure of a nanomaterial is illustrated by lithium intercalation into TiO_2−B. Both bulk and nanotube forms of TiO_2−B act as hosts for Li intercalation, but the nanotubes can store significantly more lithium, $Li_{0.98}TiO_2$−B, compared with $Li_{0.71}TiO_2$−B for the bulk material, and the rate of Li insertion/removal is higher for the nanotubes.[14] Such differences cannot be explained by the simple scaling of surface area/particle size alone: differences between nanotubes and bulk TiO_2−B must be important. The distortion of the ideal (bulk) TiO_2−B crystal structure that is involved in forming the nanotubes results in a continuous increase in the interatomic distances extending radially outward across the tube wall. The distances in the outer half of the tube are greater than those in the ideal structure, resulting in wider bottlenecks within the channels for Li^+ ion transport, consistent with a higher rate of Li^+ intercalation. The increased dimensions render many sites in the structure that were previously inaccessible to Li^+, e.g., tetrahedral sites between edge-sharing TiO_6 octahedra, now accessible, consistent with a higher maximum lithium composition. Detailed correlation is beyond the scope of the paper, but the differences in structure and properties between bulk and nanotubes cannot be coincidental.

3. Concluding Remarks

We have shown that, by using the Debye equation for X-ray scattering, it is possible to describe the powder X-ray diffraction pattern for nanotubes, including the severe *hkl*-dependent peak broadening/distortions that arise due to the bending of the crystal structure into a nanotube with a wall thickness of only a few nanometers. The method yields the deformed crystal structure of a nanotube. Unlike most established approaches, the present method makes no recourse to symmetry and does not require the separation of Bragg and non-Bragg scattering or a description of the strain and particle size broadening by specific peak-shaped functions, all factors which complicate the analysis of such severely distorted powder diffraction patterns by established methods. The shape, size, and orientation of the ordered structural unit within the nanotube are also obtained as a natural consequence of the approach. In addition, a modification of the Debye method, taking account of preferred orientation, a feature that is common to one- and two-dimensional nanomaterials, has been described. The advantage of established crystallographic methods for structure elucidation, in general, is that they reduce computational complexity by invoking translational symmetry. It is for nanomaterials, where the symmetry is most severely compromised, that the Debye approach offers the greatest benefit. Fortunately, such materials also comprise fewer atoms in a typical scattering domain, rendering this relatively computationally expensive approach tractable using modern personal computers. The method is of general applicability to nanomaterials, with the potential of providing unprecedented detail of the structure, especially for nanostructured materials such as nanotubes, nanoflakes, and nanobelts, where the structure has to deform as it bends or distorts to accommodate the particular nanomorphology, in contrast to simple zero-dimensional nanoparticles. As illustrated above, knowing the exact structure of nanomaterials provides a basis for understanding their unique properties.

Acknowledgment. P.G.B. is indebted to the EPSRC for financial support.

JA8028334